

## Article

# Grant Report on the Transcranial near Infrared Radiation and Cerebral Blood Flow in Depression (TRIADE) Study

Dan V. Iosifescu <sup>1,2,\*</sup>, Katherine A. Collins <sup>1</sup>, Aura Hurtado-Puerto <sup>3</sup>, Molly K. Irvin <sup>1,2</sup>, Julie A. Clancy <sup>3,4</sup>, Allison M. Sparpana <sup>1,2</sup>, Elizabeth F. Sullivan <sup>1,2</sup>, Zamfira Parincu <sup>1</sup>, Eva-Maria Ratai <sup>4</sup>, Christopher J. Funes <sup>3,5</sup>, Akila Weerasekera <sup>4</sup>, Jacek P. Dmochowski <sup>6</sup> and Paolo Cassano <sup>3,4,7,8</sup>

<sup>1</sup> Nathan Kline Institute for Psychiatric Research, Orangeburg, NY 10962, USA

<sup>2</sup> Department of Psychiatry, New York University Grossman School of Medicine, New York, NY 10016, USA

<sup>3</sup> Department of Psychiatry, Harvard Medical School, Boston, MA 02115, USA

<sup>4</sup> Department of Radiology, Harvard Medical School, Massachusetts General Hospital, Boston, MA 02114, USA

<sup>5</sup> Department of Psychiatry, Division of Neuropsychiatry, Massachusetts General Hospital, Boston, MA 02114, USA

<sup>6</sup> City University of New York, New York, NY 10017, USA

<sup>7</sup> Department of Psychiatry, Depression Clinical and Research Program, Massachusetts General Hospital, Boston, MA 02114, USA

<sup>8</sup> Department of Psychiatry, Center for Anxiety and Traumatic Stress Disorders, Massachusetts General Hospital, Boston, MA 02114, USA

\* Correspondence: dan.iosifescu@nki.rfmh.org

**Abstract:** We report on the rationale and design of an ongoing National Institute of Mental Health (NIMH) sponsored R61-R33 project in major depressive disorder (MDD). Current treatments for MDD have significant limitations in efficacy and side effect burden. There is a critical need for device-based treatments in MDD that are efficacious, well-tolerated, and easy to use. This project focuses on the adjunctive use of the transcranial photobiomodulation (tPBM) with near-infrared (NIR) light for the treatment of MDD. tPBM with NIR light penetrates robustly into the cerebral cortex, stimulating the mitochondrial respiratory chain, and also significantly increases cerebral blood flow (CBF). In the R61 phase, we will conduct target engagement studies to demonstrate dose-dependent effects of tPBM on the prefrontal cortex (PFC) CBF, using the increase in fMRI blood-oxygenation-level-dependent (BOLD) signal levels as our Go/No-go target engagement biomarker. In the R33 phase, we will conduct a randomized clinical trial of tPBM vs. sham in MDD to establish the target engagement and evaluate the association between changes in the biomarker (BOLD signal) and changes in clinical symptoms, while also collecting important information on antidepressant effects, safety, and tolerability. The study will be done in parallel at New York University/the Nathan Kline Institute (NYU/NKI) and at Massachusetts General Hospital (MGH). The importance of this study is threefold: 1. it targets MDD, a leading cause of disability worldwide, which lacks adequate treatments; 2. it evaluates tPBM, which has a well-established safety profile and has the potential to be safe in at-home administration; and 3. it uses fMRI BOLD changes as a target engagement biomarker. If effects are confirmed, the present study will both support short-term clinical development of an easy to scale device for the treatment of MDD, while also validating a biomarker for the development of future, novel modulation strategies.

**Keywords:** major depressive disorder (MDD); transcranial; photobiomodulation; neuromodulation; antidepressant; functional MRI (fMRI); blood-oxygenation-level-dependent (BOLD) signal; low level light therapy; laser



**Citation:** Iosifescu, D.V.; Collins, K.A.; Hurtado-Puerto, A.; Irvin, M.K.; Clancy, J.A.; Sparpana, A.M.; Sullivan, E.F.; Parincu, Z.; Ratai, E.-M.; Funes, C.J.; et al. Grant Report on the Transcranial near Infrared Radiation and Cerebral Blood Flow in Depression (TRIADE) Study. *Photonics* **2023**, *10*, 90. <https://doi.org/10.3390/photonics10010090>

Received: 29 November 2022

Revised: 23 December 2022

Accepted: 25 December 2022

Published: 13 January 2023



**Copyright:** © 2023 by the authors. Licensee MDPI, Basel, Switzerland. This article is an open access article distributed under the terms and conditions of the Creative Commons Attribution (CC BY) license (<https://creativecommons.org/licenses/by/4.0/>).

## 1. Significance *The Unmet Need*

One of the leading causes of disability worldwide, Major Depressive Disorder (MDD), affects more than 16% of the US population during their lifetime [1,2]. Existing antide-

pressants, traditionally considered first-line treatment options, are only partially effective and can have burdensome side effects [3,4]. Despite antidepressants' availability, one third of patients do not achieve remission after multiple treatments [5] and experience frequent relapses [6].

One option for individuals who do not respond to or tolerate antidepressants are neuromodulation strategies, which include the FDA-approved electroconvulsive therapy (ECT), transcranial magnetic stimulation (rTMS), and vagus nerve stimulation (VNS), as well as the experimental transcranial direct current stimulation (tDCS), magnetic seizure therapy (MST), and deep brain stimulation (DBS) [7]. While ECT and VNS are FDA-approved and have demonstrated efficacy, they are invasive—requiring anesthesia and securing airways (ECT) or surgical implantation (VNS), creating risk of perioperative and postoperative complications. Thus, for the benefits of treatment to outweigh the risk of complication, these treatments are usually reserved for the most refractory patients. rTMS is a less invasive option for patients with a wider range of depression severity, but its practicality can be limiting—it is extremely costly and requires multiple clinic visits. Alternatively, transcranial photobiomodulation (tPBM) is a safe, non-invasive, and effective neuromodulation strategy that may be well tolerated and could potentially be used by patients at home, significantly decreasing cost and clinic visits.

## 2. Transcranial Photobiomodulation

tPBM is a novel neuromodulation strategy based on non-retinal exposure to light at specific wavelengths. tPBM with near-infrared radiation (NIR) has shown promising early results for the treatment of neuropsychiatric disorders [8]. Although tPBM offers clear advantages and has the potential to increase accessibility for individuals with MDD due to its ease of use [9], affordability, and safety, there is no consensus on the optimal dose irradiance for central nervous system (CNS) disorders, a necessary step before large-scale studies demonstrating efficacy.

## 3. tPBM Penetration in the Brain

NIR undergoes exponential decay of the photon flux as it travels through tissues. Nevertheless, a small but significant fraction of the light delivered to the scalp reaches the cortex. Depending on parameters used, the distribution of the therapeutic dose (sufficient energy deposition for therapeutic effects) might vary from only the most superficial cortex to the whole cortical width, always in proximity of the light source [10–12]. While therapeutic NIR penetration varies based on wavelength [13,14], light source [light emitting diodes (LED) or laser] [15], pulsing [16], and intensity [13,15], a 2% to 3% penetration rate of NIR is attainable at target prefrontal cortex (PFC) regions. This corresponds to an NIR penetration of ~2 cm of intervening skin, skull, meninges, cerebral spinal fluid (CSF), and brain. The NIR fluence (energy density, J/cm<sup>2</sup>) at the skin surface—necessary to reach target areas of the brain therapeutically—is both safe and well tolerated. It is feasible to attain an NIR fluence on the human brain equivalent to the fluence inducing neurological benefits in animal models [17]. Figure 1 presents the spatial aspects of light absorption at the tPBM irradiation dose used in our preliminary data [18] in a realistic head model. tPBM NIR with laser devices has good penetration. NIR (808 nm) was detected 4 cm below the skin in unfixed cadaver brains ( $n = 8$ ) with a 5 W laser; the penetration at 808 nm (NIR) wavelength was superior to the 940 (NIR) and 660 nm (red) light [14]. Additionally, a 15 W laser produced a 2.9% penetration of NIR (810 nm) at 3 cm from skin surface of sheep heads [15]. The penetration for LED devices has been more variable [13,15] which supports our decision to use lasers for this application.

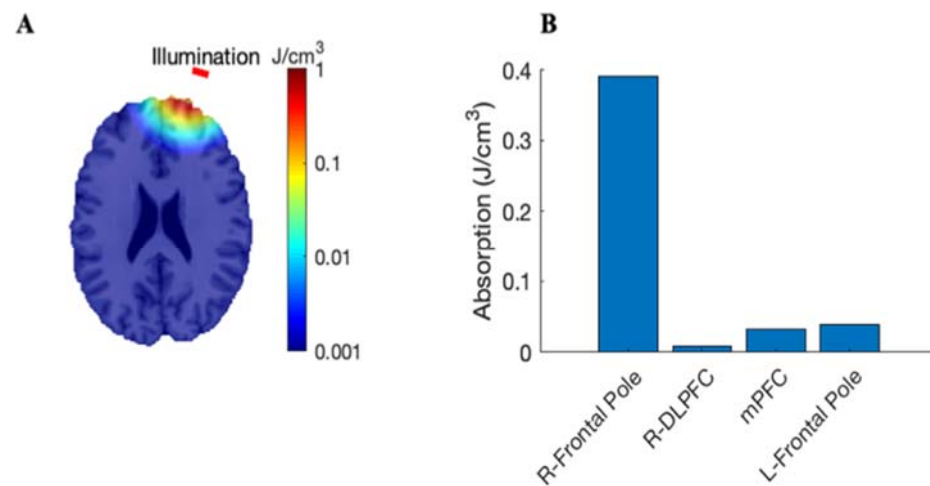


**Figure 1.** (A) Simulated light absorption in a template head (“Colin27”) when targeting the right frontal pole. Light propagation through the heterogeneous head volume was simulated using the Monte Carlo Multi-Layer (MCML) technique after assigning the appropriate optical properties to the head model and computing the energy absorbed at each location [18]. The displayed axial slice matches the site of illumination (red bar). The absorption spans three orders of magnitude and decays rapidly in both depth and lateral directions. (B) The absorption at the targeted structure (R-Frontal Pole) approaches  $0.4 \text{ J/cm}^3$ , while being limited to less than  $0.05 \text{ J/cm}^3$  in non-targeted regions such as the right dorsolateral prefrontal cortex (R-DLPFC), medial prefrontal cortex (mPFC), and left frontal pole (L-Frontal Pole).

#### 4. Cellular Mechanisms of tPBM

The NIR delivered through tPBM is absorbed by a mitochondrial enzyme and chromophore, cytochrome c oxidase (CCO), and is only minimally dissipated as thermal energy [17,19]. The peak absorption of light energy by CCO occurs at four different wavelengths; one of these peaks is 812–846 nm [20], overlapping with the wavelengths with best brain penetration described above.

Results in cellular and animal models indicate that tPBM can enhance mitochondrial activity. NIR delivers energy to the CCO and stimulates the mitochondrial respiratory chain leading to increased adenosine triphosphate (ATP) production [19,21,22]. This is relevant for MDD, which is associated with hypometabolism in specific brain areas [23–26] and mitochondrial dysfunction [27–31]. In addition, NIR can improve mitochondrial activity by promoting the dissociation of nitric oxide (NO) from the CCO, releasing the binding site for oxygen, and restoring oxidative phosphorylation [17]. The released NO may also act as a local vasodilator [32]. A study on isolated mitochondria also reported increased RNA and protein synthesis after irradiation with a low-level laser (632.8 nm) [33].

Animal research suggests that tPBM might also exert, via its impact on mitochondria, beneficial effects on several other pathophysiological mechanisms implicated in MDD, such as oxidative stress [34–38], neuroinflammation [39–43], and deficits in neuroplasticity and brain derived neurotrophic factor (BDNF) [44–46]. NIR can induce short bursts of reactive oxygen species (ROS) leading to the activation of antioxidant mechanisms and the activation of the transcription factor nuclear factor  $\kappa$ B (NF- $\kappa$ B), resulting in decreased overexpression of the inducible form of nitric oxide synthase (iNOS) and reduction of oxidative stress [32,47,48]. In animal models, NIR light (600 to 1000 nm) reduced neuroinflammation by decreasing proinflammatory cytokines such as IL-6, TNF- $\alpha$ , IL-1 $\beta$ , and IL-8 [49–51], and decreasing the infiltration of macrophages, activated microglia, and T lymphocytes to the CNS [51]. In animal studies, tPBM also stimulated neurogenesis and neuroprotective mechanisms in models of neuronal injury, possibly mediated by increased BDNF and by inhibition of GSK-3 $\beta$  and pro-apoptotic molecules [32,52–59].

## 5. Mechanisms of Action of tPBM in MDD

Multiple pre-clinical studies support the efficacy of tPBM, in single or repeated administration, on animal models of depression, such as the forced swim test [55,60–62], tail suspension test [55,61], mild chronic stress [63,64], and the reserpine-induced depression [60]. In several of these studies the antidepressant effects were associated with biological effects related to mitochondrial stimulation, such as increased ATP biosynthesis, mitochondrial complex IV expression, activity in the PFC [61], and increased hippocampal neurogenesis [62]. All clinical studies using tPBM for MDD reported in the literature aimed to modulate the forebrain, consistent with the dysfunction of the PFC associated with MDD [65]. In pilot studies with open designs, NIR was associated with an antidepressant response after a single administration [66] or repeated (six) administrations [67]. Our recent randomized control trial (RCT) showed tPBM was more efficacious than sham in 21 MDD subjects receiving bilateral tPBM at 823 nm or sham directed on dorsolateral PFC (dlPFC) [electroencephalography (EEG) sites F3 and F4] twice-a-week for 8 weeks [68]. Another study suggested that tPBM paired with a cognitive therapy may be effective in MDD [69]. All these studies measured acute, short-term effects; only one case report described persistence of effects over 9 months of repeated administration in a subject with MDD [70].

## 6. Effects of tPBM on Cerebral Blood Flow

In vivo, tPBM has robust and immediate effects on cerebral blood flow (CBF). In rats, tPBM at 660 nm with an LED device (9 mW/cm<sup>2</sup>) was associated with increased oxygen consumption in the frontal cortex [71], while in mice, NIR (808 nm) tPBM with laser (1.6 W/cm<sup>2</sup>) resulted in 30% increased CBF [72]. In healthy humans, tPBM with a 3.4 W laser (1064 nm) led to increased concentration of oxygenated hemoglobin [73]. In elderly women specifically, tPBM with a 0.2 W LED (627 nm) increased blood flow in the middle cerebral and basilar arteries [74]. In chronic traumatic brain injury (TBI) patients, tPBM with a 3.3 W LED device (629 and 850 nm) increased CBF (measured by SPECT) [75].

Our preliminary data [18] show an immediate increase in CBF in the medial frontal gyrus (MFG) regions of interest (ROIs) [measured as blood-oxygenation-level-dependent (BOLD) signal on functional magnetic resonance imaging (fMRI)] in healthy volunteers exposed to 808 nm laser NIR. This makes the impact of tPBM on CBF an ideal model for target engagement for this neuromodulation strategy.

The impact of tPBM on cortical excitability may result in increased functional connectivity in the default mode network (DMN) [76]. tPBM also has a dose-dependent modulatory effect on cortical excitability. An open study applying a pulsed low-level laser to the motor cortex with 905 nm wavelength and a peak irradiance of 50 mW/cm<sup>2</sup> for five minutes found significantly smaller motor evoked potentials (MEP) 20 min after irradiation [77]. Similarly, a controlled study applied a laser of 810 nm with a power density of 500 mW/cm<sup>2</sup> during 10 min over the motor cortex. There was a significant decrease in MEP amplitudes in the group receiving active stimulation compared to the control group. This difference was sustained 30 min after stimulation concluded [78]. In contrast, a controlled study using an 820 nm laser beam over the motor cortex at 310 mW/cm<sup>2</sup> for four minutes found an increase in MEP amplitude of up to 40% in the active versus sham arm. The difference in MEP amplitudes was significant at 10, 15, and 20 min after conclusion of stimulation [79].

## 7. Clinical Effects of tPBM on MDD

Two studies, conducted by our team at MGH, suggest that tPBM is feasible and safe in patients with MDD. In the first study [67], six sessions of adjunct tPBM NIR (810 nm, irradiance 700 mW/cm<sup>2</sup>, similar to the higher dose tested in the present study) delivered to PFC twice a week for three weeks in four MDD subjects led to a decrease in depressive symptoms [mean Hamilton Depression Rating Scale (HAM-D<sub>17</sub>) scores decreased from 19.8 ± 4.4 to 13 ± 5.35, *p* = 0.004]. tPBM at the high dose was well tolerated without any

serious adverse events (SAEs). In the double-blind, sham-controlled study [68], 16 sessions of adjunct tPBM NIR (823 nm, irradiance  $36.2 \text{ mW/cm}^2$ , similar to the lower dose used in the present study) delivered to PFC twice a week for eight weeks in MDD subjects led to a significantly greater decrease in depressive scores in the NIR-group vs. sham (HAM-D<sub>17</sub> decrease with NIR =  $15.7 \pm 4.41$  vs. sham =  $6.1 \pm 7.86$ ;  $p = 0.031$ ). tPBM was well tolerated with no SAEs. Of note, our clinical pilot study [68] demonstrated a large effect size (Cohen's  $d = 1.5$ ) and reached significance with 13 subjects completing the treatment (Figure 2). These data support the potential clinical efficacy of tPBM. Additionally, a recently published report [80] from our group suggests that tPBM at very low energy and irradiance may not have robust clinical antidepressant efficacy. This result highlights the importance of dose finding studies, such as the one presented in this report, to determine the optimal irradiance dose.

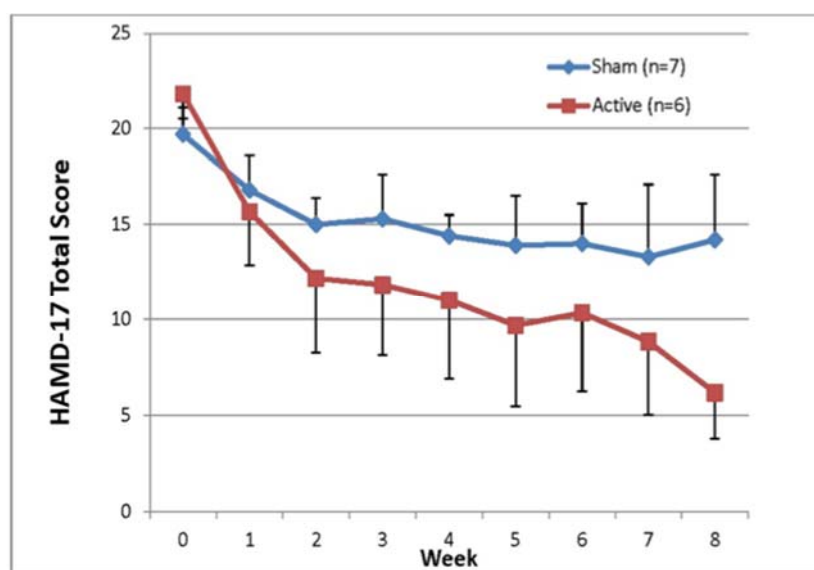


**Figure 2.** Antidepressant effect of tPBM versus sham [35], 2x/week over 8 weeks. (Figure re-used with permission from Photobiomodulation, Photomedicine, and Laser Surgery).

## 8. Safety and Tolerability of tPBM

The safety of one session of tPBM was evaluated in three large RCTs with a pooled sample of 1410 subjects with stroke [81–83]. No significant difference in the rate of adverse effects were observed between the group receiving laser NIR (808 nm; 5 W,  $700 \text{ mW/cm}^2$ ) or sham. No SAEs were found in our review of the literature [84]. In two open studies with few (one and six) tPBM sessions, no treatment-emergent side-effects were reported [66,67]. A clinical trial with 16 sessions reported some mild side-effects, such as frequent insomnia, “seeing vivid colors”, “an ashtray-like taste”, and irritable mood [68]. A pooled data analysis of three studies on tPBM for mood and anxiety disorders confirmed good tolerability in this population [9]. Other potential risks relate to inappropriate administration. Laser devices have a potential risk of retinal lesions when used improperly; this is mitigated with appropriate safety eye gear and procedures. tPBM has minimal risk for thermal injury. Even when used in much higher doses, such as for the treatment of TBI, participants’ skin temperature did not increase to more than  $30 \text{ }^\circ\text{C}$  and cooled down rapidly once tPBM was over. Patients did not experience any discomfort, only slight skin warming [85].

## 9. Preliminary Data on the Effect of tPBM on CBF (Measured with fMRI-BOLD)

In a prior study, we collected fMRI data from 20 healthy volunteers undergoing tPBM in the resting state [18]. To disambiguate the effects of CBF from those of blood oxygenation, we employed a multi-echo magnetic resonance (MR) sequence [86]. Subjects’ brain activity (BOLD signal) was acquired continuously for 30 min, with tPBM applied

for 10 min beginning at minute 11. Stimulation was delivered with a laser (808 nm), with an irradiance dose of  $318 \text{ mW/cm}^2$  (similar to the middle dose used in the current study) and a spot size of  $1 \text{ cm}^2$  to the right forehead (standard EEG electrode location “Fp2”). Whole-brain voxel-wise statistical Chow tests [87] were conducted separately at each echo of the group-averaged BOLD to detect changes during and after tPBM, relative to the pre-stimulation baseline. During tPBM, we found a significant modulation of early-echo (13 ms) BOLD in a cluster of 214 voxels in the right MFG, 24 mm from the site of light incidence (Figure 3). The most robust BOLD signal increase from baseline was detected at echo 1 (associated with a large effect size: Cohen’s  $d = 1.54$ ). At echo 2 (34 ms), a cluster of 154 voxels in the right MFG, 22.4 mm from incidence, was also found to exhibit significant BOLD increase from baseline. Four smaller clusters were detected at echo 3 (56 ms), including one in the right superior frontal gyrus (SFG), 22.5 mm from incidence. Importantly, the effect of tPBM on the early-echo BOLD outlasted the stimulation: a cluster of 218 voxels centered in the MFG (at 28.7 mm from incidence) had significant increases in BOLD post stimulation. The presence of significant BOLD increases at all echos, including the early-echo, which is insensitive to blood oxygenation, suggests that CBF (and not merely oxygenation) was robustly increased during and after tPBM (Figure 4). These data support the validity and the feasibility of using quantitative changes in fMRI-BOLD as a biomarker for target engagement during tPBM, and guide design decisions for this study.

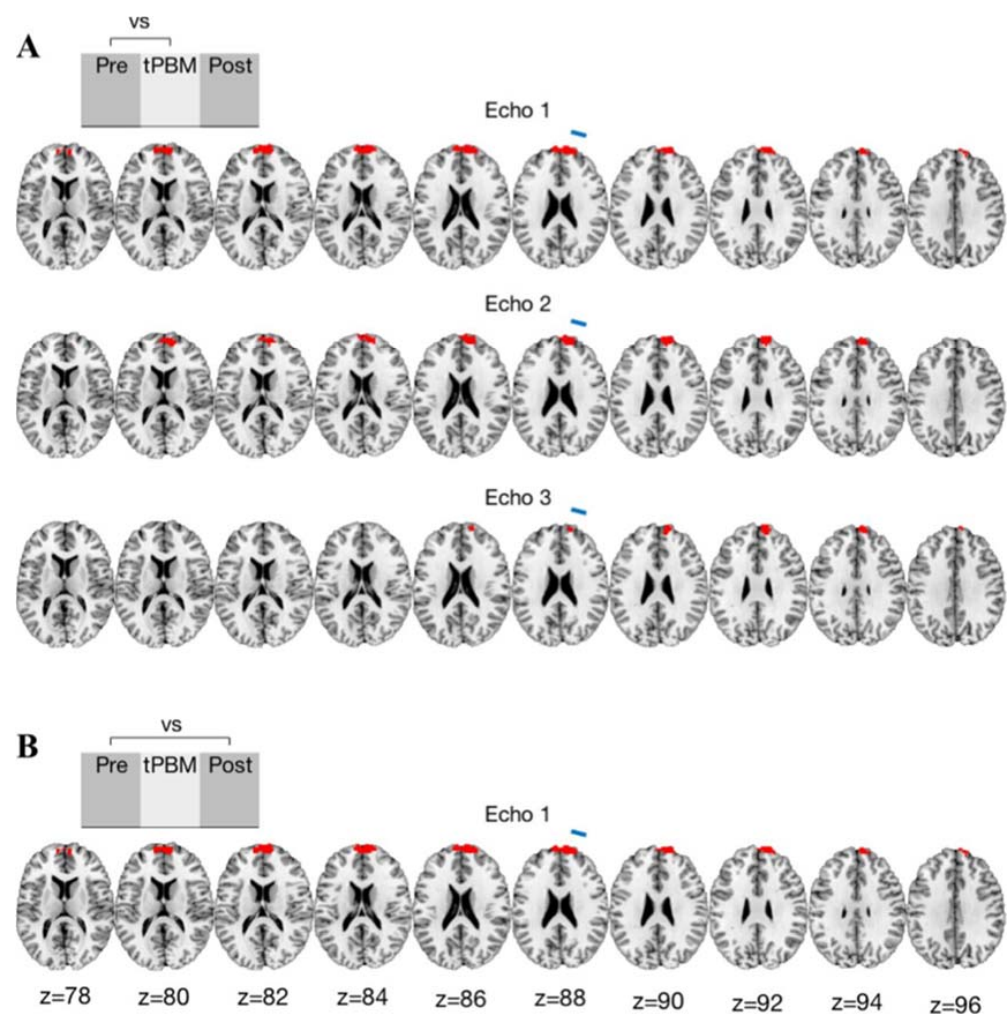


**Figure 3.** tPBM modulates fMRI-BOLD during and after stimulation. (A) An acute modulation of BOLD at prefrontal regions was observed at all 3 echos. (B) A lasting effect post tPBM was detected in echo 1. “Z” represents the axial slice position.

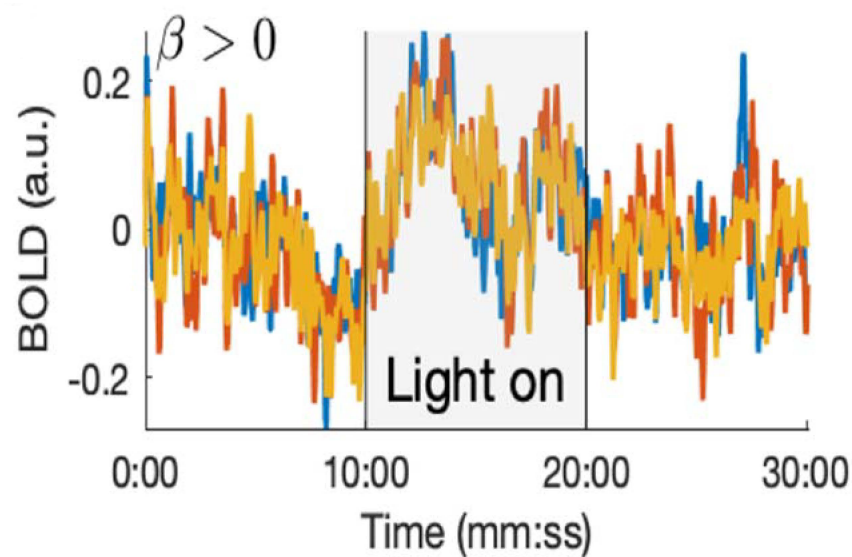


**Figure 4.** Time series of BOLD changes after tPBM was applied to the right forehead 10 min. into a 30 min. BOLD scan [18]. The duration of stimulation was 10 min. (grey area). The colored time series indicate the subject-averaged BOLD (shown here in a ROI corresponding to the right medial frontal gyrus, MFG) at echos 1 (blue, 13 ms), 2 (red, 34 ms), and 3 (orange, 55 ms). A rapid increase in the BOLD was observed shortly after stimulation onset, while a second peak emerged later in the 10 min. stimulation window.

## 10. Innovation

The current project is innovative because: 1. it tests tPBM with NIR, an innovative technology with a well-established safety profile; 2. it is the first study to evaluate the dose-dependent effects of tPBM on changes in CBF in MDD subjects, as measured with the BOLD fMRI signal, as a state-of-the-art target engagement biomarker; and 3. it is the first study to evaluate the effects of tPBM on brain temperature in humans *in vivo* in conjunction with clinical symptoms, providing further insights on safety and dose-dependent mechanisms of action.

The limitations of current treatments in MDD are well documented. Preliminary data suggest tPBM could be a novel treatment strategy in MDD. This study pilots a novel measurement of changes in BOLD fMRI signal as a marker of changes in CBF in the search for the optimal tPBM dose, with the long-term goal of transforming clinical practice for patients with MDD. If the effects of optimal tPBM dose are confirmed in repeated administration, the present study will both support clinical development of an innovative neuromodulation strategy and offer ideal methods to test its application in other neuropsychiatric conditions.

## 11. Approach

This two-phase (R61/R33) study is being conducted at New York University (NYU), the Nathan Kline Institute for Psychiatric Research (NKI), and the Massachusetts General Hospital (MGH). In the first (R61) phase, we are seeking objective evidence of dose-dependent target engagement by tPBM, operationalized as change in CBF in the PFC, quantified with the fMRI BOLD signal [18]. Successful demonstration of target engagement will identify the optimal tPBM dose and serve as the Go criterion for transition to the second (R33) phase, during which we will conduct an RCT of tPBM vs. sham in MDD to establish the target engagement and evaluate the association between changes in the biomarker (BOLD signal increase during tPBM) and changes in clinical symptoms, while also collecting important information on antidepressant effects, safety, and tolerability.

## 12. Specific Aims (SA)

### 12.1. Aim 1 (R61): To Demonstrate Target Engagement by tPBM in MDD

We will utilize the fMRI BOLD signal change during tPBM (808 nm over 24 cm<sup>2</sup>) at three irradiance doses (High dose: Pulse wave (PW), average irradiance ~300 mW/cm<sup>2</sup>, 600 s, 40 Hz, 33% duty cycle, ~4.3 kJ total energy; Medium dose: Continuous Wave (CW), ~300 mW/cm<sup>2</sup> irradiance, 333 s, ~2.4 kJ total energy; Low dose: CW, ~50 mW/cm<sup>2</sup> irradiance; 1200 s, ~1.4 kJ total energy) relative to sham as our objective evidence of target engagement. Thirty MDD subjects will each receive all three tPBM doses as well as sham treatment (approximately one week apart, in random order) during fMRI scanning.

There is no formal hypothesis testing in the R61 phase. We have previously observed large effect size (Cohen's  $d = 1.54$ ) changes in BOLD in the MFG ROI after a single administration of tPBM (at 318 mW/cm<sup>2</sup>) [18]. In our clinical pilot study, significant, large effect size improvements in depressive symptoms were reported in MDD after eight weeks (Cohen's  $d = 1.5$ ,  $n = 21$ ) [68]. Given these preliminary results, we anticipate that the tPBM dose with the largest associated increase in BOLD in the MFG ROIs (the target) will be associated with at least a medium effect size (the effect of tPBM on the target will be of magnitude Cohen's  $d \geq 0.5$ ). If we observe a dose-dependent effect on BOLD in the MFG ROIs, and if the effect of the optimal dose on the BOLD signal is of magnitude at least Cohen's  $d = 0.5$ , the R61 will validate BOLD fMRI as a robust biomarker of target engagement for tPBM and act as a Go signal for the progression to the R33 phase. In contrast, if none of the tPBM doses yield reliable BOLD increases, this will fail the putative mechanism (No Go). Additional important safety milestones will include the lack of SAEs and lack of significant increase in brain temperature, as measured with MR Thermometry.

### 12.2. Aim 2 (R33): To Confirm Target Engagement at the tPBM Irradiance Dose Identified in R61 and Determine the Relationship between Changes in Target Biomarker and Clinical Symptoms

#### Aim 3 (R33): To Collect Information about the Antidepressant Effect of tPBM in MDD

In the R33 study, 60 subjects with MDD will be randomized to an 8-week treatment with tPBM or sham. Before baseline and after primary outcome assessments, we will also assess BOLD changes during open label tPBM to incorporate R61 biomarkers. We will formally test two hypotheses: 1. tPBM affects the target (BOLD change) among MDD subjects; and 2. changes in the target are associated with changes in depression symptoms. In addition, we will estimate the size of the effect of tPBM at the optimal dose on depression symptoms. The R33 will strongly inform decisions about whether tPBM has the potential to substantially reduce depressive symptoms in MDD. If successful, the project will encourage future clinical testing of this low-cost, accessible, and user-friendly intervention in subjects with MDD and other mood disorders. In addition, the project will support the use of BOLD signal changes as a biomarker for testing future neuromodulation strategies in MDD.

## 13. R61 Phase

### 13.1. Study Schedule

After informed consent, subjects undergo psychiatric screening, a blood draw for laboratory tests (if deemed necessary by study PI), urinalysis, drug screen, pregnancy test for people of child-bearing potential, and a physical examination. Clinical screening measures include: 1. Montreal Cognitive Assessment (MoCA); 2. Mini International Neuropsychiatric Interview (MINI); 3. Columbia Suicide Severity Rating Scale (C-SSRS); and 4. Inventory of Depressive Symptomology–Clinician-Administered version (IDS-C). Additionally, study staff record skin color via the New Immigrant Survey–Skin Color Scale (NIS-SCS). We gather this data for use as a potential covariate in analyses as skin color can affect absorption of NIR.

Eligible subjects return for four fMRI + tPBM/sham sessions. At each visit, a study clinician or clinical research coordinator administers the following safety and clinical assessments: 1. Montgomery-Åsberg Depression Rating Scale (MADRS); 2. Clinical Global Impression Severity and Improvement scales (CGI-S and CGI-I); and 3. C-SSRS. Addition-

ally, subjects complete the following self-rated forms: 1. Anxiety Symptoms Questionnaire (ASQ); 2. Quality of Life in Neurological Disorders, Cognitive Section (Neuro-QoL); 3. Positive and Negative Affect Schedule (PANAS); 4. Potential Confounders Questionnaire (PCQ); 5. Quality of Life, Enjoyment, and Satisfaction Questionnaire–Short Form (Q-LESQ-SF); 6. Systematic Assessment for Treatment Emergent Events (SAFTEE); 7. Symptoms of Depression Questionnaire (SDQ); 8. Perceived Blinding Questionnaire (PBQ); and 9. tPBM Self-Report Questionnaire (TSRQ). The PBQ and TSRQ are rated after tPBM administration. A study clinician monitors subjects for depressive worsening, adverse events (AEs), or changes to concomitant medications within 24 h of every visit (Table 1).

**Table 1.** The schedule of events and procedures at each study visit.

Study Phase	Screen (R61 & R33)	R61: t-PBM/sham + fMRI	R61: Follow-Up	R33: Baseline	R33: Treatment	R33: Primary Outcome	R33: Final Visit or ET	Event Based
Week	−2	1–4	5	1	1–8	8	9	
Visit #	1	2–5	6	2	3–15	16	17	
Consent	X							
AE Form		X	X	X	X	X	X	X
ASQ		X	X	X	X	X	X	
ATRQ	X							
CGI-I/S		X	X	X	X	X	X	
Concomitant Meds	X	X	X	X	X	X	X	X
C-SSRS	X	X	X	X	X	X	X	X
Demographic data	X							
fMRI + t-PBM/sham		X		X		X		
IDS-C	X							
Inclusion/exclusion	X							
MADRS		X	X	X	X	X	X	
Medical history, Physical exam	X							
MINI	X							
MoCA	X							
MRI Safety Checklist	X	X		X		X		
Neuro-QoL		X	X	X	X	X	X	
NIS-SCS	X							
PANAS		X	X					
PBQ		X				X	X	
PCQ		X	X	X	X	X	X	
Pregnancy test	X							
QLESQ		X	X	X	X	X	X	
Safety labs	X							
SAFTEE-SI		X	X	X	X	X	X	X
SDQ		X	X	X	X	X	X	
t-PBM/sham					X (2/WEEK)			
TSRQ		X		X	X	X		
Urine drug screen	X							
Vital signs	X	X		X	X	X	X	X

AE = Adverse Events form; ASQ = Anxiety Symptoms Questionnaire; ATRQ = Antidepressant Treatment Response Questionnaire; CGI = Clinical Global Impression Scale; C-SSRS = Columbia Suicide Severity Rating Scale; IDS-C = Inventory of Depressive Symptomatology, clinician version; MADRS = Montgomery Asberg Depression Rating Scale; MINI = Mini-International Neuropsychiatric Interview; MoCA = Montreal Cognitive Assessment; Neuro-QoL = Quality of Life in Neurological Disorders, Cognitive Section; NIS-SCS = NIS Skin Color Scale; PANAS = The Positive and Negative Affect Scale; PBQ = Perceptions of Blinding Questionnaire; PCQ = Potential Confounders Questionnaire; QLESQ = Quality of Life, Enjoyment, and Satisfaction Questionnaire; SAFTEE-SI = The Systematic Assessment for Treatment Emergent Effects–Systematic Inquiry; SDQ = Symptoms of Depression Questionnaire; TSRQ = t-PBM Self-Report Questionnaire.

A remote follow-up visit with a licensed medical professional occurs approximately one week after completion of the four study visits. Participants are evaluated for safety assessment and clinical care dispositions. Safeguards ensure that participants with severe, worsening depression and/or suicidal ideation will be offered appropriate care.

13.2. Device

Subjects receive each of four tPBM/sham doses (“low,” “medium,” and “high” vs. sham, parameters specified in Table 2) approximately one week apart during fMRI scanning. Dose order is randomized.

**Table 2.** Parameters of the four tPBM irradiance doses.

Parameters	Dose			
	High	Middle	Low	Sham
Irradiance (mW/cm <sup>2</sup> )	~300	~300	~50	0
Exposure time (s)	600	333	1200	0
Average Fluence (J/cm <sup>2</sup> )	~180	~100	~60	0
Total energy (kJ)	~4.3	~2.4	~1.4	0
Wave Mode	Pulsed	Continuous	Continuous	N/A
Duty Cycle (%)	33	N/A	N/A	N/A
Pulse Rate (Hz)	~40	N/A	N/A	N/A
NIR source	Laser	Laser	Laser	N/A
Wavelength	808 nm	808 nm	808 nm	N/A
Area of exposure	24 cm <sup>2</sup>	24 cm <sup>2</sup>	24 cm <sup>2</sup>	N/A
Anatomical targets	F4, F3	F4, F3	F4, F3	F4, F3

The tPBM-2.0 is an investigational device based on LiteCure’s LightForce® EXPi Deep Tissue Laser Therapy™ System. For the investigational study, the EXPi System’s beam delivery—Empower™, is modified to non-invasively deliver NIR to subjects diagnosed with MDD. The modified system is also configured to provide sham treatment. The device is manufactured and supplied by LiteCure LLC, New Castle, DE, USA.

The tPBM-2.0 is considered a Class II medical device per 21 CFR 890.5500 and 878.4810 and is manufactured per 21 CFR 820. It utilizes a laser diode source with a maximum continuous (CW) output of ≤30 Watts at a wavelength of 808 nanometers (nm) and nominal beam diameter of 40 mm at the outside aperture.

The tPBM-2.0 operates in one of four modes (see Table 2). The device’s behavior, performance/output of all visible and audible indicators, including the graphic user interface, is identical for all modes, which differ only with respect to the parameters of laser emission. Since the laser radiation emitted during NIR mode is invisible to the naked eye, the active and sham modes are indistinguishable from one another. Participants will be blinded to the order in which they experience each of the four modes. The treatment mode administered at each session will depend on a pre-determined randomization scheme.

The tPBM-2.0 consists of a therapeutic laser console (that produces laser energy as NIR) and an optical delivery system consisting of a flexible, double-sheathed optical fiber connected to a custom helmet (cap). The cap is configured to deliver NIR light to EEG sites F4 and F3 (or in close proximity if covered by hair), covering a total surface treatment area of approximately 24 cm<sup>2</sup> (12 cm<sup>2</sup> × 2). It also includes laser safety eye ware with an optical density rating >5.0 at 808 nm. The tPBM-2.0 is a nonsignificant risk device.

### 13.3. Imaging Procedures

We use similar MRI procedures to our pilot [18] which demonstrated the feasibility of our methods. Imaging is performed on 3T Siemens Trio MRI scanners utilizing 12-channel transmit/receive head coils at either NKI or MGH. As a safety measure, all subjects wear protective eye goggles in addition to the study device during scanning. After localization, we acquire structural images with a T1-weighted MPRAGE sequence (FOV 256 mm, in plane resolution  $256 \times 256$ , 192 1 mm slices, TR = 2500 ms, TE = 3.5 ms, TI = 1200 ms, flip angle 8 degrees).

We collect multi-echo functional MRI pre-, during, and post-tPBM/sham. The parameters for the pre- and post- sequences are: 2174 Hz/Px bandwidth, TR = 2500 ms, TE1 = 12.8 ms, TE2 = 33.41 ms, TE3 = 54.02 ms, voxel size 2.5 mm  $\times$  2.5 mm  $\times$  2.5 mm, acquisition duration 10:30 min, 60 slices, multiband acceleration factor = 2, flip angle 65 degrees. Parameters for stimulation sequences are identical to those of the pre- and post-sequences for the high dose. For the medium dose, the time of acquisition is 6:15 min. For the low dose, the time of acquisition is 20:40 min.

In addition to structural and functional MR data collection, we also collect pre- and post- tPBM/sham single voxel H-MR spectroscopy data to assess the brain temperature fluctuations. Water suppressed spectra were acquired using a Point RESolved Spectroscopy (PRESS) sequence with the following parameters: TR = 2000 ms, TE = 30 ms, bandwidth = 2000 Hz, vector size = 1024 [88]. A voxel with  $30 \times 30 \times 15$  mm<sup>3</sup> dimensions was placed on the left frontal lobe, in the cortical region immediately beneath the laser outlet. Scans were acquired in 4-blocks, each with 32 averages (total NA = 128) for post-motion correction purposes. Total acquisition time was 4:48 min.

### 13.4. Imaging Preprocessing

Preprocessing of MRI and fMRI data is performed with the AfNI software package [89], scripted in Matlab (Mathworks, Natick, MA, USA). All participants' anatomical images are skull-stripped and registered to the Talairach atlas. We then perform slice-time correction, motion-correction, and co-registration of the functional BOLD scans of each echo, TR, and participant. The BOLD signals are then smoothed to a full-width half-maximum (FWHM) of 4 mm and z-scored at every voxel. Further denoising is performed by regressing out the first three principal components of the white matter signal, as this step has been shown in our preliminary data to effectively reduce residual motion artifacts. The two ROIs have been pre-defined as two clusters of 200 voxels in the MFG, bilateral, with coordinates in agreement with our preliminary data [18]. The preprocessed and denoised BOLD signals are averaged across the voxels within each ROI.

To combine and compare data across sites, we ensured the data acquisition methods and parameters are identical. Human BOLD signal relative changes (expressed as ratios relative to the pre-treatment baseline) are highly comparable without even intensity calibration since scanner-specific effects simply "cancel out" in the ratios. Thus, intravoxel relative BOLD signal changes which will be implemented in this study are self-calibrating and ensure fMRI data comparability across site and time.

The R61 will be conducted over 24 months, with fMRI data analyzed on a rolling basis, allowing for a two-month analysis period/decision of Go/No Go for the R33.

## 14. R33 Phase

### 14.1. Study Schedule

Sixty MDD subjects will be randomized to tPBM (at the dose selected in the R61) or sham. After informed consent, participants will complete the screening visit. Subjects will undergo identical screening procedures to the R61. Those meeting enrollment criteria will return within approximately two weeks for a baseline visit, during which they will receive an open-label dose of active tPBM during fMRI to evaluate its impact on BOLD signal before randomization. Patients will return for 16 tPBM sessions (without fMRI), scheduled to take place approximately twice per week for 8 weeks. Half of the visits will include

safety and clinical assessments. After the conclusion of the study treatment and primary clinical outcomes (week 8), another open-label tPBM dose will be administered during fMRI to assess possible changes in BOLD signal reactivity after eight weeks of tPBM. The final visit (week 9) will include post-study safety evaluation.

Subjects will be randomized 1:1 to NIR or sham. Study population, structural and functional MR protocols, and safety and clinical assessments will be identical to those selected for the R61 phase (Figure 5).

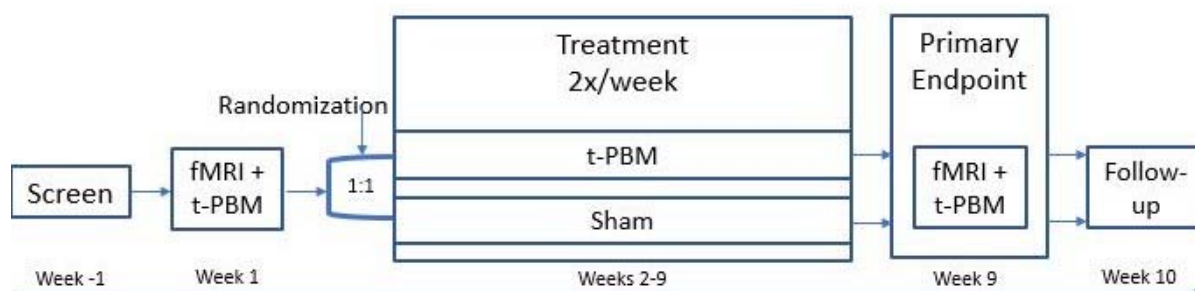


**Figure 5.** Schema of the R33 phase of the study.

The R33 phase will determine the viability of further development of tPBM therapy. We will consider 1. dose-dependent BOLD increase during tPBM administration; 2. compared to sham, the BOLD increase at the optimal dose will have an effect size of Cohen's  $d \geq 0.5$ ; and 3. absence of safety concerns related to the tPBM (operationalized as a discontinuation rate due to side effects of  $<20\%$  and an absence of any SAEs attributed to tPBM).

#### 14.2. Imaging

Imaging will be performed on 3T Siemens Trio MRI scanners utilizing 12-channel transmit/receive head coils at either NKI or MGH. As a safety measure, all subjects will wear protective eye goggles in addition to the study device during scanning.

All enrolled subjects will undergo neuroimaging studies using identical protocols, with uniform implementation across sites. We will acquire structural and functional images, as described above. Spectroscopy will not be collected. Consistent with our preliminary data, the results of the first echo (12.8 ms) will be used for computing the BOLD change [18].

### 15. Data Management

The Innovative Clinical Research Solutions (ICRS) group at NKI is the Data Coordinating Center (DCC) and conducts all data management and data quality assurance activities. To ensure the completeness and integrity of all study data, ICRS provides a comprehensive data management methodology combined with strong planning, control, and coordination with study research staff. ICRS developed all study Case Report Forms (CRFs) to standardize data collection [based on CRFs used in previous National Institute of Mental Health (NIMH) studies]. A comprehensive web-based data acquisition and management system, "Acquire," was programmed to process, edit, and store all study data in a centralized database. ICRS personnel implement rigorous data editing and validation using the Acquire system, and they review and monitor the completeness and accuracy of study data throughout the study. Final data clean-up will be completed shortly after the last data collection time point and a final locked study database will be provided to the study statistician for analyses.

### 16. Data Analysis and Power Assumptions

Before any statistical techniques are applied, the distribution of all variables will be investigated using descriptive statistics and outliers will be examined. Where necessary, non-parametric statistical methods will be used rather than relying on distributional assumptions. Since the main goal of R61/R33 is to obtain evidence about the mechanism of

action, the feasibility of implementation, and the potential for efficacy of novel treatment strategies that, if warranted, will be tested in future confirmatory studies, the emphasis of the statistical analysis will be on estimation [with effect sizes and confidence intervals (CIs)] rather than on hypothesis testing. Where formal hypothesis testing is employed, significance will be judged at 5% level, two-sided.

#### 16.1. SA1 (R61): To Demonstrate Target Engagement by tPBM in MDD

For each subject at each tPBM dose, we will obtain the BOLD signal change measure at the specified ROI. This measure will be modeled as a function of dose (considered a categorical variable with four levels) using mixed effects models [90], including random subject intercepts to account for the potentially correlated measures on the same subject. Since the doses will be presented to subjects in a random order, the initial model will also include order of the dose (a continuous variable) and all interactions between the dose and the order. If there is evidence for an interaction effect between dose and order, this effect will be investigated to understand how the dose effect varies as a function of week of treatment; in such cases, effect size of the tPBM doses will be estimated using only the data when the dose was given in the first week. If there is no interaction between dose and order, the order variable and the interactions will be omitted, and the resulting model will be used to estimate the mean BOLD signal measures at each dose and the differences between each active tPBM dose and sham.

We anticipate no more than 20% dropout during the four-week intervention, which would result in about 24 observations at each of the four doses. This sample size would allow us to estimate the effect size of the optimal dose within 0.37 units (80% CI), or 0.57 (95% CI), which is considered an adequate level of evidence for the goals of the R61 mechanism. The analytic method is mixed effects model which will provide somewhat better power than the one reported above under worst-case scenario. Of note, we observed a large effect size for BOLD signal changes ( $d = 1.54$ ) during tPBM in the right MFG in our preliminary data [18] in healthy controls.

#### 16.2. SA2 (R33): To Confirm Target Engagement at the tPBM Irradiance Dose Identified in R61 and Determine the Relationship between Changes in Target Biomarker and Clinical Symptoms

**Hypothesis 1:** *At the optimal dose determined in R61, tPBM will be associated with significantly larger BOLD signal increases compared to sham. The two treatment groups (tPBM and sham) will be compared with respect to their maximum BOLD signal increase from baseline using a linear regression. The maximum post-tPBM BOLD signal increase will be modeled as a function of treatment (tPBM vs. sham), controlling for the pre-administration BOLD signal.*

**Detectable effects:** Given the sample size of  $n = 30$  per group, we will be able to detect with 80% power at 5% significance level (2-sided test) an effect size of Cohen's  $d \geq 0.75$ . The study is designed to detect a large effect for the following reasons: 1. assuming a moderately strong association between changes in the target and clinical outcomes, the effects of tPBM on the target need to be fairly large in order to translate into clinically meaningful effects on the clinical symptoms; and 2. in our pilot study, we observed a very large effect of tPBM on BOLD signal in the prefrontal cortex ( $d = 1.54$ ). Depending on the findings in R61, the sample size of the RCT in R33 might be changed: for example, if in R61 the effect of tPBM on BOLD signal at the selected dose is very large, we might appropriately decrease the sample size in the R33 and aim at detecting effects of  $d = 1.0$  instead.

**Hypothesis 2:** *Improvement in depression severity (MADRS scores) during the eight-week tPBM treatment will be correlated with larger BOLD signal increases (measured at randomization). We will use a linear regression, modeling the outcome (severity of depression) at week 8 post-randomization as a function of change (from pre- to during tPBM) in BOLD at randomization and controlling for the severity of symptoms at randomization. Testing this hypothesis is equivalent to testing the significance of the regression coefficient for change in BOLD. We will explore whether the relationship of interest is the same under both treatments (tPBM and sham) by including an*

*interaction term between treatment and maximum BOLD signal change at randomization and evaluating its magnitude.*

**Detectable effects:** The power of the test based on the linear regression model described above depends on the correlation ( $\rho$ ) between the outcome at week 8 and the symptom severity at randomization, with larger correlation increasing the power. Given the total sample size of 60, there is 80% power (2-sided test,  $\alpha = 0.05$ ) to detect the following effects: if  $\rho = 0$ , we can detect a relationship between changes in target and outcome that corresponds to 13% explained variance in the outcome by changes in the target; if  $\rho = 0.2$  we can detect an effect corresponding to 12% explained variance in the outcome; if  $\rho = 0.5$ , the detectable effect corresponds to 10% explained variance. Allowing for 20% dropout, resulting in missing post-treatment data for 12 subjects, the detectable effects are as follows: Explained variance of 16%, 14%, and 12% for  $\rho = 0, 0.2,$  and  $0.5,$  respectively.

### 16.3. SA3 (R33): To Collect Information about the Antidepressant Effect of tPBM in MDD

We will study the course of clinical symptoms (depression severity, using MADRS) over the 8-week RCT and will compare and contrast the outcome trajectories between the two treatment groups (tPBM vs. sham). This will supply evidence regarding overall effects of tPBM and timing of emergence of the effects. If our hypotheses are confirmed, this information will be used for designing an adequately powered study establishing the efficacy of tPBM for MDD. We will collect information on the feasibility and acceptability of tPBM, and the timing, course, and magnitude of the expected effects. The analyses will depend on the distributions of the collected data. For example, if there is evidence for linear changes of symptoms over time, the post-randomization symptoms will be modeled as functions of treatment, time, and treatment by time interactions and controlling for the values of the outcome at baseline, using linear mixed effects models, with random subject intercepts and slopes. Rather than testing, however, we will estimate the effects and provide 95% confidence intervals for 1. differences in mean rates of symptom change over time; and 2. differences of mean symptoms at different time points. The precision of the estimated contrasts between the two treatment groups will depend on the models used for estimation, which would depend on the distribution of the outcomes data, including the correlations between the repeated observations over time on the same subject, as well as on the particular contrast (difference in means at a given time, or difference between slopes of symptoms change, etc.). For example, with 30 subjects per group, the difference between the mean values at week 8 of treatment can be estimated with 95% CI within 0.2–0.4 standard deviation of the symptoms at randomization. Of note, large effect sizes for improvements in depressive symptoms with tPBM were reported in our pilot MDD study ( $d = 1.5$ ) [68]; the proposed sample size allows sufficient power to detect such large effects with 2-sided significance test with  $\alpha = 0.05$ .

The biomarker (change in BOLD with tPBM) collected at the last treatment session will allow exploratory analyses of changes in baseline CBF, as well in the reactivity of CBF, after repeated tPBM doses in MDD.

## 17. Discussion

tPBM with NIR has been demonstrated in previous studies to be a safe, low cost, easily self-administered treatment with promising early results in neuropsychiatric disorders. This two-part study aims to first (R61) determine the optimal dose of tPBM to achieve neural target engagement (assessed with BOLD fMRI), and to then (R33) utilize the dose with the largest impact on CBF in repeated administration to further establish clinical utility. Specific hypotheses for the R33 include 1. tPBM affects target BOLD change among subjects with MDD; and 2. changes in the target are associated with changes in depression symptoms. This study is particularly significant for a wide variety of patients with MDD who either do not respond to or cannot feasibly afford or tolerate existing treatments. The procedures outlined here can also be applicable to future studies to test similar hypotheses with many other neuropsychiatric disorders.

**Author Contributions:** Conceptualization, D.V.I. and P.C.; methodology, J.P.D., K.A.C. and A.H.-P. (fMRI) and E.-M.R., A.W. (MRS); writing—original draft preparation, M.K.I., J.A.C., A.M.S., E.F.S., Z.P., C.J.F.; writing—review and editing, M.K.I., J.A.C., A.M.S., E.F.S., Z.P., C.J.F.; supervision, D.V.I. and P.C.; project administration, D.V.I. and P.C.; funding acquisition, D.V.I. and P.C. All authors have read and agreed to the published version of the manuscript.

**Funding:** This study is financed through grant R61/R33 MH122647 from the US National Institute of Mental Health (Drs. Iosifescu and Cassano).

**Institutional Review Board Statement:** The study protocol was approved by the institutional Review Board of NYU Grossman School of Medicine.

**Informed Consent Statement:** This is a report describing an upcoming research study. All participants in the study will provide IRB-approved, informed consent.

**Data Availability Statement:** The data generated in this study will be uploaded to the NIH data archive and will be available for sharing to interested investigators, in agreement with NIH policy.

**Conflicts of Interest:** In the last 5 years, Dr. Iosifescu has received consulting honoraria from Alkermes, Allergan, Angelini, Axsome, Biogen, Centers for Psychiatric Excellence, Clexio, Global Medical Education, Jazz, Lundbeck, Otsuka, Precision Neuroscience, Relmada, Sage, and Sunovion and research support (through his academic institution) from Alkermes, AstraZeneca, Brainsway, LiteCure, NeoSync, Otsuka, Roche, and Shire. Dr. Cassano consulted for Janssen Research and Development and for Niraxx Light Therapeutics Inc; was funded by PhotoThera Inc., LiteCure LLC, and Cerebral Sciences Inc to conduct studies on transcranial photobiomodulation; is a shareholder of Niraxx Light Therapeutics Inc; and has filed several patents related to the use of near infrared light in psychiatry. The other authors have nothing to disclose.

## References

1. Kessler, R.C.; Berglund, P.; Demler, O.; Jin, R.; Koretz, D.; Merikangas, K.R.; Rush, A.J.; Walters, E.E.; Wang, P.S. The Epidemiology of Major Depressive Disorder. *JAMA* **2003**, *289*, 3095. [[CrossRef](#)] [[PubMed](#)]
2. Ferrari, A.J.; Charlson, F.J.; Norman, R.E.; Patten, S.B.; Freedman, G.; Murray, C.J.L.; Vos, T.; Whiteford, H.A. Burden of Depressive Disorders by Country, Sex, Age, and Year: Findings from the Global Burden of Disease Study 2010. *PLoS Med.* **2013**, *10*, e1001547. [[CrossRef](#)]
3. Cassano, P.; Fava, M. Tolerability Issues during Long-Term Treatment with Antidepressants. *Ann. Clin. Psychiatry* **2004**, *16*, 15–25. [[CrossRef](#)]
4. Kennedy, S.H.; Lam, R.W.; McIntyre, R.S.; Tourjman, S.V.; Bhat, V.; Blier, P.; Hasnain, M.; Jollant, F.; Levitt, A.J.; MacQueen, G.M.; et al. Canadian Network for Mood and Anxiety Treatments (CANMAT) 2016 Clinical Guidelines for the Management of Adults with Major Depressive Disorder. *Can. J. Psychiatry* **2016**, *61*, 540–560. [[CrossRef](#)] [[PubMed](#)]
5. Rush, A.J.; Warden, D.; Wisniewski, S.R.; Fava, M.; Trivedi, M.H.; Gaynes, B.N. STAR\*D: Revising Conventional Wisdom. *CNS Drugs* **2009**, *23*, 627–647. [[PubMed](#)]
6. Sinyor, M.; Schaffer, A.; Levitt, A. The Sequenced Treatment Alternatives to Relieve Depression (STAR\*D) Trial: A Review. *Can. J. Psychiatry* **2010**, *55*, 126–135. [[CrossRef](#)]
7. Milev, R.V.; Giacobbe, P.; Kennedy, S.H.; Blumberger, D.M.; Daskalakis, Z.J.; Downar, J.; Modirrousta, M.; Patry, S.; Vila-Rodriguez, F.; Lam, R.W.; et al. Canadian Network for Mood and Anxiety Treatments (CANMAT) 2016 Clinical Guidelines for the Management of Adults with Major Depressive Disorder. *Can. J. Psychiatry* **2016**, *61*, 561–575. [[CrossRef](#)]
8. Hamblin, M.R. Shining Light on the Head: Photobiomodulation for Brain Disorders. *BBA Clin.* **2016**, *6*, 113–124. [[CrossRef](#)]
9. Cassano, P.; Norton, R.; Caldieraro, M.A.; Vahedifard, F.; Vizcaino, F.; McEachern, K.M.; Iosifescu, D. Tolerability and Safety of Transcranial Photobiomodulation for Mood and Anxiety Disorders. *Photonics* **2022**, *9*, 507. [[CrossRef](#)]
10. Yue, L.; Humayun, M.S. Monte Carlo Analysis of the Enhanced Transcranial Penetration Using Distributed Near-Infrared Emitter Array. *J. Biomed. Opt.* **2015**, *20*, 088001. [[CrossRef](#)]
11. Yuan, Y.; Cassano, P.; Pias, M.; Fang, Q. Transcranial Photobiomodulation with Near-Infrared Light from Childhood to Elderliness: Simulation of Dosimetry. *Neurophoton* **2020**, *7*, 015009. [[CrossRef](#)]
12. Cassano, P.; Tran, A.P.; Katnani, H.; Bleier, B.S.; Hamblin, M.R.; Yuan, Y.; Fang, Q. Selective Photobiomodulation for Emotion Regulation: Model-Based Dosimetry Study. *Neurophotonics* **2019**, *6*, 015004. [[CrossRef](#)]
13. Jagdeo, J.R.; Adams, L.E.; Brody, N.I.; Siegel, D.M. Transcranial Red and Near Infrared Light Transmission in a Cadaveric Model. *PLoS ONE* **2012**, *7*, e47460. [[CrossRef](#)] [[PubMed](#)]
14. Tedford, C.E.; DeLapp, S.; Jacques, S.; Anders, J. Quantitative Analysis of Transcranial and Intraparenchymal Light Penetration in Human Cadaver Brain Tissue. *Lasers Surg. Med.* **2015**, *47*, 312–322. [[CrossRef](#)] [[PubMed](#)]
15. Henderson, T.A.; Morris, L. Near-Infrared Photonic Energy Penetration: Can Infrared Phototherapy Effectively Reach the Human Brain? *Neuropsychiatr. Dis. Treat* **2015**, *11*, 2191. [[CrossRef](#)] [[PubMed](#)]

16. Hashmi, J.T.; Huang, Y.-Y.; Sharma, S.K.; Kurup, D.B.; de Taboada, L.; Carroll, J.D.; Hamblin, M.R. Effect of Pulsing in Low-Level Light Therapy. *Lasers Surg. Med.* **2010**, *42*, 450–466. [[CrossRef](#)]
17. Chung, H.; Dai, T.; Sharma, S.K.; Huang, Y.-Y.; Carroll, J.D.; Hamblin, M.R. The Nuts and Bolts of Low-Level Laser (Light) Therapy. *Ann. Biomed. Eng.* **2012**, *40*, 516–533. [[CrossRef](#)]
18. Dmochowski, G.; Dmochowski, J. Increased Blood Flow and Oxidative Metabolism in the Human Brain by Transcranial Laser Stimulation. *bioRxiv* **2018**. [[CrossRef](#)]
19. Mochizuki-Oda, N.; Kataoka, Y.; Cui, Y.; Yamada, H.; Heya, M.; Awazu, K. Effects of Near-Infra-Red Laser Irradiation on Adenosine Triphosphate and Adenosine Diphosphate Contents of Rat Brain Tissue. *Neurosci. Lett.* **2002**, *323*, 207–210. [[CrossRef](#)]
20. Karu, T.I.; Kolyakov, S.F. Exact Action Spectra for Cellular Responses Relevant to Phototherapy. *Photomed. Laser Surg.* **2005**, *23*, 355–361. [[CrossRef](#)]
21. Oron, U.; Ilic, S.; de Taboada, L.; Streeter, J. Ga-As (808 Nm) Laser Irradiation Enhances ATP Production in Human Neuronal Cells in Culture. *Photomed. Laser Surg.* **2007**, *25*, 180–182. [[CrossRef](#)] [[PubMed](#)]
22. Yu, W.; Naim, J.O.; McGowan, M.; Ippolito, K.; Lanzafame, R.J. Photomodulation of Oxidative Metabolism and Electron Chain Enzymes in Rat Liver Mitochondria. *Photochem. Photobiol.* **1997**, *66*, 866–871. [[CrossRef](#)] [[PubMed](#)]
23. Drevets, W. Functional Anatomical Correlates of Antidepressant Drug Treatment Assessed Using PET Measures of Regional Glucose Metabolism. *Eur. Neuropsychopharmacol.* **2002**, *12*, 527–544. [[CrossRef](#)] [[PubMed](#)]
24. Kennedy, S.H.; Konarski, J.Z.; Segal, Z.V.; Lau, M.A.; Bieling, P.J.; McIntyre, R.S.; Mayberg, H.S. Differences in Brain Glucose Metabolism between Responders to CBT and Venlafaxine in a 16-Week Randomized Controlled Trial. *Am. J. Psychiatry* **2007**, *164*, 778–788. [[CrossRef](#)]
25. Mayberg, H.S.; Brannan, S.K.; Tekell, J.L.; Silva, J.A.; Mahurin, R.K.; McGinnis, S.; Jerabek, P.A. Regional Metabolic Effects of Fluoxetine in Major Depression: Serial Changes and Relationship to Clinical Response. *Biol. Psychiatry* **2000**, *48*, 830–843. [[CrossRef](#)] [[PubMed](#)]
26. Videbech, P. PET Measurements of Brain Glucose Metabolism and Blood Flow in Major Depressive Disorder: A Critical Review. *Acta Psychiatr. Scand* **2000**, *101*, 11–20. [[CrossRef](#)]
27. Bansal, Y.; Kuhad, A. Mitochondrial Dysfunction in Depression. *Curr. Neuropharmacol.* **2016**, *14*, 610–618. [[CrossRef](#)]
28. Hroudová, J.; Fišar, Z.; Kitzlerová, E.; Zvěřová, M.; Raboch, J. Mitochondrial Respiration in Blood Platelets of Depressive Patients. *Mitochondrion* **2013**, *13*, 795–800. [[CrossRef](#)]
29. Karabatsiakos, A.; Böck, C.; Salinas-Manrique, J.; Kolassa, S.; Calzia, E.; Dietrich, D.E.; Kolassa, I.-T. Mitochondrial Respiration in Peripheral Blood Mononuclear Cells Correlates with Depressive Subsymptoms and Severity of Major Depression. *Transl. Psychiatry* **2014**, *4*, e397. [[CrossRef](#)]
30. Morava, É.; Kozicz, T. Mitochondria and the Economy of Stress (Mal)Adaptation. *Neurosci. Biobehav. Rev.* **2013**, *37*, 668–680. [[CrossRef](#)]
31. Iosifescu, D.V.; Bolo, N.R.; Nierenberg, A.A.; Jensen, J.E.; Fava, M.; Renshaw, P.F. Brain Bioenergetics and Response to Triiodothyronine Augmentation in Major Depressive Disorder. *Biol. Psychiatry* **2008**, *63*, 1127–1134. [[CrossRef](#)] [[PubMed](#)]
32. de Freitas, L.F.; Hamblin, M.R. Proposed Mechanisms of Photobiomodulation or Low-Level Light Therapy. *IEEE J. Sel. Top. Quantum Electron.* **2016**, *22*, 348–364. [[CrossRef](#)]
33. Greco, M.; Guida, G.; Perlino, E.; Marra, E.; Quagliariello, E. Increase in RNA and Protein Synthesis by Mitochondria Irradiated with Helium-Neon Laser. *Biochem. Biophys. Res. Commun.* **1989**, *163*, 1428–1434. [[CrossRef](#)] [[PubMed](#)]
34. Eren, İ.; Naziroğlu, M.; Demirdaş, A. Protective Effects of Lamotrigine, Aripiprazole and Escitalopram on Depression-Induced Oxidative Stress in Rat Brain. *Neurochem. Res.* **2007**, *32*, 1188–1195. [[CrossRef](#)] [[PubMed](#)]
35. Ozcan, M.; Gulec, M.; Ozerol, E.; Polat, R.; Akyol, O. Antioxidant Enzyme Activities and Oxidative Stress in Affective Disorders. *Int. Clin. Pharmacol. Clin. Exp.* **2007**, *22*, 67–73. [[CrossRef](#)]
36. Sarandol, A.; Sarandol, E.; Eker, S.S.; Erdinc, S.; Vatanserver, E.; Kirli, S. Major Depressive Disorder Is Accompanied with Oxidative Stress: Short-Term Antidepressant Treatment Does Not Alter Oxidative–Antioxidative Systems. *Hum. Psychopharmacol. Clin. Exp.* **2007**, *22*, 67–73. [[CrossRef](#)]
37. Shungu, D.C.; Weiduschat, N.; Murrrough, J.W.; Mao, X.; Pillemer, S.; Dyke, J.P.; Medow, M.S.; Natelson, B.H.; Stewart, J.M.; Mathew, S.J. Increased Ventricular Lactate in Chronic Fatigue Syndrome. III. Relationships to Cortical Glutathione and Clinical Symptoms Implicate Oxidative Stress in Disorder Pathophysiology. *NMR Biomed.* **2012**, *25*, 1073–1087. [[CrossRef](#)]
38. Spanemberg, L.; Caldieraro, M.; Arrua Vares, E.; Wollenhaupt de Aguiar, B.; Yuri Kawamoto, S.; Parker, G.; Pio Fleck, M.; Kauer-SantAnna, M.; Galvao, E. Biological Differences between Melancholic and Nonmelancholic Depression Subtyped by the CORE Measure. *Neuropsychiatr. Dis. Treat* **2014**, *10*, 1523. [[CrossRef](#)]
39. Dowlati, Y.; Herrmann, N.; Swardfager, W.; Liu, H.; Sham, L.; Reim, E.K.; Lanctôt, K.L. A Meta-Analysis of Cytokines in Major Depression. *Biol. Psychiatry* **2010**, *67*, 446–457. [[CrossRef](#)]
40. Köhler, C.A.; Freitas, T.H.; Maes, M.; de Andrade, N.Q.; Liu, C.S.; Fernandes, B.S.; Stubbs, B.; Solmi, M.; Veronese, N.; Herrmann, N.; et al. Peripheral Cytokine and Chemokine Alterations in Depression: A Meta-Analysis of 82 Studies. *Acta Psychiatr. Scand* **2017**, *135*, 373–387. [[CrossRef](#)]
41. Liu, Y.; Ho, R.C.-M.; Mak, A. Interleukin (IL)-6, Tumour Necrosis Factor Alpha (TNF- $\alpha$ ) and Soluble Interleukin-2 Receptors (SIL-2R) Are Elevated in Patients with Major Depressive Disorder: A Meta-Analysis and Meta-Regression. *J. Affect. Disord* **2012**, *139*, 230–239. [[CrossRef](#)] [[PubMed](#)]

42. Yoshimura, R.; Hori, H.; Ikenouchi-Sugita, A.; Umene-Nakano, W.; Ueda, N.; Nakamura, J. Higher Plasma Interleukin-6 (IL-6) Level Is Associated with SSRI- or SNRI-Refractory Depression. *Prog. Neuropsychopharmacol. Biol. Psychiatry* **2009**, *33*, 722–726. [[CrossRef](#)]
43. Lindqvist, D.; Janelidze, S.; Hagell, P.; Erhardt, S.; Samuelsson, M.; Minthon, L.; Hansson, O.; Björkqvist, M.; Träskman-Bendz, L.; Brundin, L. Interleukin-6 Is Elevated in the Cerebrospinal Fluid of Suicide Attempters and Related to Symptom Severity. *Biol. Psychiatry* **2009**, *66*, 287–292. [[CrossRef](#)] [[PubMed](#)]
44. Autry, A.E.; Monteggia, L.M. Brain-Derived Neurotrophic Factor and Neuropsychiatric Disorders. *Pharmacol. Rev.* **2012**, *64*, 238–258. [[CrossRef](#)]
45. Duman, R. Pathophysiology of Depression and Innovative Treatments: Remodeling Glutamatergic Synaptic Connections. *Dialogues Clin. Neurosci.* **2014**, *16*, 11–27. [[CrossRef](#)]
46. Molendijk, M.L.; Spinhoven, P.; Polak, M.; Bus, B.A.A.; Penninx, B.W.J.H.; Elzinga, B.M. Serum BDNF Concentrations as Peripheral Manifestations of Depression: Evidence from a Systematic Review and Meta-Analyses on 179 Associations (N = 9484). *Mol. Psychiatry* **2014**, *19*, 791–800. [[CrossRef](#)] [[PubMed](#)]
47. Rizzi, C.F.; Mauriz, J.L.; Freitas Corrêa, D.S.; Moreira, A.J.; Zettler, C.G.; Filippin, L.I.; Marroni, N.P.; González-Gallego, J. Effects of Low-Level Laser Therapy (LLLT) on the Nuclear Factor (NF)-KB Signaling Pathway in Traumatized Muscle. *Lasers Surg. Med.* **2006**, *38*, 704–713. [[CrossRef](#)]
48. Chludzińska, L.; Ananicz, E.; Jarosawska, A.; Komorowska, M. Near-Infrared Radiation Protects the Red Cell Membrane against Oxidation. *Blood Cells Mol. Dis.* **2005**, *35*, 74–79. [[CrossRef](#)]
49. Araki, H.; Imaoka, A.; Kuboyama, N.; Abiko, Y. Reduction of Interleukin-6 Expression in Human Synoviocytes and Rheumatoid Arthritis Rat Joints by Linear Polarized Near Infrared Light (SuperLizer) Irradiation. *Laser Ther.* **2011**, *20*, 293–300. [[CrossRef](#)]
50. Yamaura, M.; Yao, M.; Yaroslavsky, I.; Cohen, R.; Smotrich, M.; Kochevar, I.E. Low Level Light Effects on Inflammatory Cytokine Production by Rheumatoid Arthritis Synoviocytes. *Lasers Surg. Med.* **2009**, *41*, 282–290. [[CrossRef](#)]
51. Anders, J. The Potential of Light Therapy for Central Nervous System Injury and Disease. *Photomed. Laser Surg.* **2009**, *27*, 379–380. [[CrossRef](#)]
52. Giuliani, A.; Lorenzini, L.; Gallamini, M.; Massella, A.; Giardino, L.; Calzà, L. Low Infra Red Laser Light Irradiation on Cultured Neural Cells: Effects on Mitochondria and Cell Viability after Oxidative Stress. *BMC Complement. Altern. Med.* **2009**, *9*, 8. [[CrossRef](#)]
53. Rojas, J.C.; Lee, J.; John, J.M.; Gonzalez-Lima, F. Neuroprotective Effects of Near-Infrared Light in an In Vivo Model of Mitochondrial Optic Neuropathy. *J. Neurosci.* **2008**, *28*, 13511–13521. [[CrossRef](#)]
54. Wong-Riley, M.T.T.; Liang, H.L.; Eells, J.T.; Chance, B.; Henry, M.M.; Buchmann, E.; Kane, M.; Whelan, H.T. Photobiomodulation Directly Benefits Primary Neurons Functionally Inactivated by Toxins. *J. Biol. Chem.* **2005**, *280*, 4761–4771. [[CrossRef](#)]
55. Ando, T.; Xuan, W.; Xu, T.; Dai, T.; Sharma, S.K.; Kharkwal, G.B.; Huang, Y.-Y.; Wu, Q.; Whalen, M.J.; Sato, S.; et al. Comparison of Therapeutic Effects between Pulsed and Continuous Wave 810-Nm Wavelength Laser Irradiation for Traumatic Brain Injury in Mice. *PLoS ONE* **2011**, *6*, e26212. [[CrossRef](#)]
56. Oron, A.; Oron, U.; Streeter, J.; de Taboada, L.; Alexandrovich, A.; Trembovler, V.; Shohami, E. Low-Level Laser Therapy Applied Transcranially to Mice Following Traumatic Brain Injury Significantly Reduces Long-Term Neurological Deficits. *J. Neurotrauma* **2007**, *24*, 651–656. [[CrossRef](#)]
57. Wu, Q.; Xuan, W.; Ando, T.; Xu, T.; Huang, L.; Huang, Y.-Y.; Dai, T.; Dhital, S.; Sharma, S.K.; Whalen, M.J.; et al. Low-Level Laser Therapy for Closed-Head Traumatic Brain Injury in Mice: Effect of Different Wavelengths. *Lasers Surg. Med.* **2012**, *44*, 218–226. [[CrossRef](#)]
58. Xuan, W.; Vatansver, F.; Huang, L.; Wu, Q.; Xuan, Y.; Dai, T.; Ando, T.; Xu, T.; Huang, Y.-Y.; Hamblin, M.R. Transcranial Low-Level Laser Therapy Improves Neurological Performance in Traumatic Brain Injury in Mice: Effect of Treatment Repetition Regimen. *PLoS ONE* **2013**, *8*, e53454. [[CrossRef](#)]
59. Xuan, W.; Agrawal, T.; Huang, L.; Gupta, G.K.; Hamblin, M.R. Low-Level Laser Therapy for Traumatic Brain Injury in Mice Increases Brain Derived Neurotrophic Factor (BDNF) and Synaptogenesis. *J. Biophotonics* **2015**, *8*, 502–511. [[CrossRef](#)]
60. Mohammed, H.S. Transcranial Low-Level Infrared Laser Irradiation Ameliorates Depression Induced by Reserpine in Rats. *Lasers Med. Sci.* **2016**, *31*, 1651–1656. [[CrossRef](#)]
61. Xu, Z.; Guo, X.; Yang, Y.; Tucker, D.; Lu, Y.; Xin, N.; Zhang, G.; Yang, L.; Li, J.; Du, X.; et al. Low-Level Laser Irradiation Improves Depression-Like Behaviors in Mice. *Mol. Neurobiol.* **2017**, *54*, 4551–4559. [[CrossRef](#)]
62. Tanaka, Y.; Akiyoshi, J.; Kawahara, Y.; Ishitobi, Y.; Hatano, K.; Hoaki, N.; Mori, A.; Goto, S.; Tsuru, J.; Matsushita, H.; et al. Infrared Radiation Has Potential Antidepressant and Anxiolytic Effects in Animal Model of Depression and Anxiety. *Brain Stimul.* **2011**, *4*, 71–76. [[CrossRef](#)]
63. Salehpour, F.; Rasta, S.H.; Mohaddes, G.; Sadigh-Eteghad, S.; Salarirad, S. Therapeutic Effects of 10-Hz Pulsed Wave Lasers in Rat Depression Model: A Comparison between near-Infrared and Red Wavelengths. *Lasers Surg. Med.* **2016**, *48*, 695–705. [[CrossRef](#)]
64. Wu, X.; Alberico, S.L.; Moges, H.; de Taboada, L.; Tedford, C.E.; Anders, J.J. Pulsed Light Irradiation Improves Behavioral Outcome in a Rat Model of Chronic Mild Stress. *Lasers Surg. Med.* **2012**, *44*, 227–232. [[CrossRef](#)]
65. Koenigs, M.; Grafman, J. The Functional Neuroanatomy of Depression: Distinct Roles for Ventromedial and Dorsolateral Prefrontal Cortex. *Behav. Brain Res.* **2009**, *201*, 239–243. [[CrossRef](#)]

66. Schiffer, F.; Johnston, A.L.; Ravichandran, C.; Polcari, A.; Teicher, M.H.; Webb, R.H.; Hamblin, M.R. Psychological Benefits 2 and 4 Weeks after a Single Treatment with near Infrared Light to the Forehead: A Pilot Study of 10 Patients with Major Depression and Anxiety. *Behav. Brain Funct.* **2009**, *5*, 46. [[CrossRef](#)]
67. Cassano, P.; Cusin, C.; Mischoulon, D.; Hamblin, M.R.; de Taboada, L.; Pisoni, A.; Chang, T.; Yeung, A.; Ionescu, D.F.; Petrie, S.R.; et al. Near-Infrared Transcranial Radiation for Major Depressive Disorder: Proof of Concept Study. *Psychiatry J.* **2015**, *2015*, 352979. [[CrossRef](#)]
68. Cassano, P.; Petrie, S.R.; Mischoulon, D.; Cusin, C.; Katnani, H.; Yeung, A.; de Taboada, L.; Archibald, A.; Bui, E.; Baer, L.; et al. Transcranial Photobiomodulation for the Treatment of Major Depressive Disorder. The ELATED-2 Pilot Trial. *Photomed. Laser Surg.* **2018**, *36*, 634–646. [[CrossRef](#)]
69. Disner, S.G.; Beevers, C.G.; Gonzalez-Lima, F. Transcranial Laser Stimulation as Neuroenhancement for Attention Bias Modification in Adults with Elevated Depression Symptoms. *Brain Stimul.* **2016**, *9*, 780–787. [[CrossRef](#)]
70. Caldieraro, M.A.; Sani, G.; Bui, E.; Cassano, P. Long-Term Near-Infrared Photobiomodulation for Anxious Depression Complicated by Takotsubo Cardiomyopathy. *J. Clin. Psychopharmacol.* **2018**, *38*, 268–270. [[CrossRef](#)]
71. Rojas, J.C.; Bruchey, A.K.; Gonzalez-Lima, F. Low-Level Light Therapy Improves Cortical Metabolic Capacity and Memory Retention. *J. Alzheimer's Dis.* **2012**, *32*, 741–752. [[CrossRef](#)]
72. Uozumi, Y.; Nawashiro, H.; Sato, S.; Kawauchi, S.; Shima, K.; Kikuchi, M. Targeted Increase in Cerebral Blood Flow by Transcranial Near-Infrared Laser Irradiation. *Lasers Surg. Med.* **2010**, *42*, 566–576. [[CrossRef](#)] [[PubMed](#)]
73. Tian, F.; Hase, S.N.; Gonzalez-Lima, F.; Liu, H. Transcranial Laser Stimulation Improves Human Cerebral Oxygenation. *Lasers Surg. Med.* **2016**, *48*, 343–349. [[CrossRef](#)]
74. Salgado, A.S.I.; Zângaro, R.A.; Parreira, R.B.; Kerppers, I.I. The Effects of Transcranial LED Therapy (TCLT) on Cerebral Blood Flow in the Elderly Women. *Lasers Med. Sci.* **2015**, *30*, 339–346. [[CrossRef](#)]
75. Hipkind, S.G.; Grover, F.L.; Fort, T.R.; Helffenstein, D.; Burke, T.J.; Quint, S.A.; Bussiere, G.; Stone, M.; Hurtado, T. Pulsed Transcranial Red/Near-Infrared Light Therapy Using Light-Emitting Diodes Improves Cerebral Blood Flow and Cognitive Function in Veterans with Chronic Traumatic Brain Injury: A Case Series. *Photomed. Laser Surg.* **2018**. [[CrossRef](#)]
76. Ho, M.D.; Martin, P.; Yee, M.; Koo, B.; Baker, E.; Hamblin, M.R.; Naeser, M. Increased Functional Connectivity in Default Mode Network Associated with Application of Transcranial, Light-Emitting Diodes to Treat Chronic Aphasia: Case Series. *J. Int. Neuropsychiatry* **2016**, *22*, 229.
77. Konstantinović, L.M.; Jelić, M.B.; Jeremić, A.; Stevanović, V.B.; Milanović, S.D.; Filipović, S.R. Transcranial Application of Near-Infrared Low-Level Laser Can Modulate Cortical Excitability. *Lasers Surg. Med.* **2013**, *45*, 648–653. [[CrossRef](#)]
78. Chaieb, L.; Antal, A.; Masurat, F.; Paulus, W. Neuroplastic Effects of Transcranial Near-Infrared Stimulation (TNIRS) on the Motor Cortex. *Front. Behav. Neurosci.* **2015**, *9*, 147. [[CrossRef](#)]
79. Song, P.; Han, T.; Lin, H.; Li, S.; Huang, Q.; Dai, X.; Wang, R.; Wang, Y. Transcranial Near-Infrared Stimulation May Increase Cortical Excitability Recorded in Humans. *Brain Res. Bull.* **2020**, *155*, 155–158. [[CrossRef](#)]
80. Iosifescu, D.V.; Norton, R.J.; Tural, U.; Mischoulon, D.; Collins, K.; McDonald, E.; De Taboada, L.; Foster, S.; Cusin, C.; Yeung, A.; et al. Very Low-Level Transcranial Photobiomodulation for Major Depressive Disorder: The ELATED-3 Multicenter, Randomized, Sham-Controlled Trial. *J. Clin. Psychiatry* **2022**, *83*, 21m14226. [[CrossRef](#)]
81. Hacke, W.; Schellinger, P.D.; Albers, G.W.; Bornstein, N.M.; Dahlof, B.L.; Fulton, R.; Kasner, S.E.; Shuaib, A.; Richieri, S.P.; Dilly, S.G.; et al. Transcranial Laser Therapy in Acute Stroke Treatment. *Stroke* **2014**, *45*, 3187–3193. [[CrossRef](#)] [[PubMed](#)]
82. Lampl, Y.; Zivin, J.A.; Fisher, M.; Lew, R.; Welin, L.; Dahlof, B.; Borenstein, P.; Andersson, B.; Perez, J.; Caparo, C.; et al. Infrared Laser Therapy for Ischemic Stroke: A New Treatment Strategy. *Stroke* **2007**, *38*, 1843–1849. [[CrossRef](#)] [[PubMed](#)]
83. Huisa, B.N.; Stemer, A.B.; Walker, M.G.; Rapp, K.; Meyer, B.C.; Zivin, J.A. Transcranial Laser Therapy for Acute Ischemic Stroke: A Pooled Analysis of NEST-1 and NEST-2. *Int. J. Stroke* **2013**, *8*, 315–320. [[CrossRef](#)] [[PubMed](#)]
84. Caldieraro, M.A.; Cassano, P. Transcranial and Systemic Photobiomodulation for Major Depressive Disorder: A Systematic Review of Efficacy, Tolerability and Biological Mechanisms. *J. Affect. Disord.* **2019**, *243*, 262–273. [[CrossRef](#)]
85. Henderson, T.A.; Morries, L.; Cassano, P. Treatments for Traumatic Brain Injury with Emphasis on Transcranial Near-Infrared Laser Phototherapy. *Neuropsychiatr. Dis. Treat* **2015**, *11*, 2159. [[CrossRef](#)]
86. Posse, S.; Wiese, S.; Gembris, D.; Mathiak, K.; Kessler, C.; Grosse-Ruyken, M.-L.; Elghahwagi, B.; Richards, T.; Dager, S.R.; Kiselev, V.G. Enhancement of BOLD-Contrast Sensitivity by Single-Shot Multi-Echo Functional MR Imaging. *Magn. Reson. Med.* **1999**, *42*, 87–97. [[CrossRef](#)]
87. Chow, G.C. Tests of Equality Between Sets of Coefficients in Two Linear Regressions. *Econometrica* **1960**, *28*, 591. [[CrossRef](#)]
88. Bottomley, P.A. Spatial Localization in NMR Spectroscopy in Vivo. *Ann. N. Y. Acad. Sci.* **1987**, *508*, 333–348. [[CrossRef](#)]
89. Cox, R.W. AFNI: Software for Analysis and Visualization of Functional Magnetic Resonance Neuroimages. *Comput. Biomed. Res.* **1996**, *29*, 162–173. [[CrossRef](#)]
90. Diggle, P.; Heagerty, P.; Liang, K.-Y.; Zeger, S. *Analysis of Longitudinal Data*; Oxford University Press: New York, NY, USA, 2005.

**Disclaimer/Publisher's Note:** The statements, opinions and data contained in all publications are solely those of the individual author(s) and contributor(s) and not of MDPI and/or the editor(s). MDPI and/or the editor(s) disclaim responsibility for any injury to people or property resulting from any ideas, methods, instructions or products referred to in the content.